

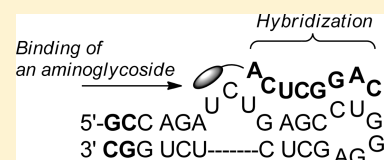
## Synthesis of Aminoglycoside-3'-Conjugates of 2'-O-Methyl Oligoribonucleotides and Their Invasion to a <sup>19</sup>F labeled HIV-1 TAR Model

Anu Kiviniemi and Pasi Virta\*

Department of Chemistry, University of Turku, FIN-20014 Turku, Finland

Supporting Information

**ABSTRACT:** The potential of aminoglycosides to induce RNA-invasion has been demonstrated. For this purpose, aminoglycoside-3'-conjugates of 2'-O-methyl oligoribonucleotides have been synthesized entirely on a solid phase. The synthesis includes an automated oligonucleotide chain elongation to solid-supported neomycin, ribostamycin, and methyl neobiosamine, and a two-step deprotection/release of the solid-supported conjugate, which allows exploitation of a simple protecting group scheme. Conjugates have been targeted to a <sup>19</sup>F labeled HIV-1 TAR RNA model (Trans Activation Response element of HIV), which allows monitoring of the invasion by <sup>19</sup>F NMR spectroscopy. A remarkably enhanced invasion, compared to that resulting from the corresponding unmodified 2'-O-methyl oligoribonucleotide (5'-CAGGCUCA-3'), has been obtained by the neomycin conjugate. The increased affinity results from a cooperative binding of the neomycin moiety and hybridization, though the invasion may also follow a mechanism, in which the first molar equivalent of the conjugate induces hybridization of the second.



### INTRODUCTION

Aminoglycosides are antibiotics, which interact with a variety of RNA targets. Binding to the ribosomal decoding site (A-site) is the basis of their bactericidal effect,<sup>1–5</sup> and comparable affinities to other RNA targets, e.g., to several ribozymes<sup>6–16</sup> and to important RNA motifs of HIV (TAR, RRE and DIS),<sup>17–20</sup> show their potential as more general RNA-targeting drugs. Aminoglycosides are also able to stabilize DNA- and RNA-triplexes, DNA-RNA hybrid triplexes, and hybrid duplexes.<sup>21–23</sup> The recognition of a certain RNA target is usually based on a bulge or an internal loop, in which the canonical base-pairing is disrupted by few mismatches.<sup>24</sup> As an example, the site-specific binding of neomycin to the HIV-1 TAR region occurs below the UCU bulge through the minor groove.<sup>25</sup> Although the nonionic interactions may play an important role in the recognition, aminoglycosides' affinity to RNA mainly originates from electrostatic interaction of their protonated amino groups with phosphodiester linkages. The binding, hence, is promiscuous, which is the main bottleneck of aminoglycoside-based RNA-targeting.<sup>24</sup> In principle, the promiscuity may be overcome by appropriate structural modifications, but conformational adaption of an RNA target upon complex formation makes development of specific ligands extremely complex.<sup>26</sup> One option to increase the specificity is the conjugation of aminoglycosides to other recognition moieties. By conjugation to oligonucleotides or PNA, the aminoglycoside's binding may be cooperatively directed by hybridization, and the specificity may be expectedly improved. In view of the antisense approach,<sup>27,28</sup> such conjugates are attractive, since the binding of the covalently attached aminoglycoside may enhance hybridization and direct the drug

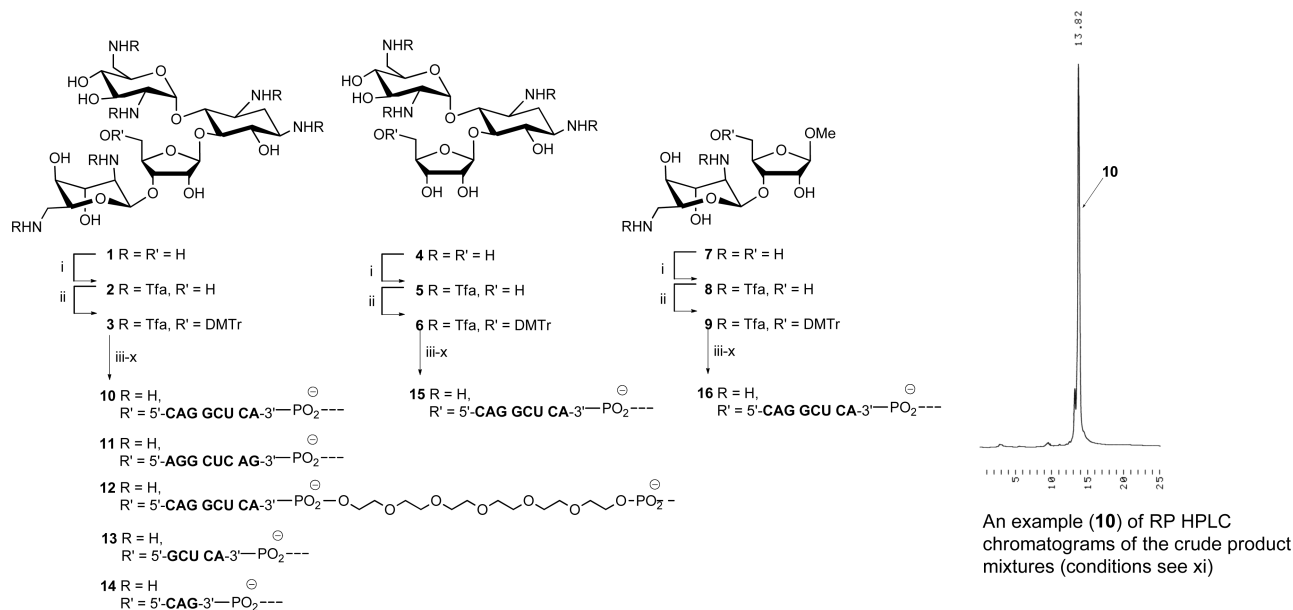
design to shorter oligonucleotide sequences. Improvements considering the cellular uptake may additionally be provided since neomycin has been shown to assist the lipid-mediated delivery of oligonucleotides.<sup>29</sup> Pioneering work for the aminoglycoside-induced antisense oligonucleotides has already been done. Neomycin has been covalently attached into an oligodeoxyribonucleotide, complementary to a seven-bases-long  $\alpha$ -sarcin loop RNA sequence, and its ability to enhance duplex formation has been studied.<sup>30</sup> A 14-mer PNA-neamine conjugate targeted to HIV-1 TAR has displayed anti-HIV-1 activity and sequence-specific metal-ion-independent cleavage of the target RNA.<sup>31,32</sup> A set of neamine- and ribostamycin-2'-O-methyl oligoribonucleotide conjugates has been prepared in order to study their nuclease activity,<sup>33</sup> and DNA-duplex stabilization has been obtained by 4'-C-conjugated paromamine.<sup>34,35</sup> It is worth noting that conjugation of neamine with dinucleotides has been reported to remarkably decrease affinity to HIV-1 TAR RNA, due to electrostatic repulsion between the phosphates, whereas conjugates of the corresponding PNA show about 2-fold binding affinities compared to that of neamine.<sup>36</sup>

HIV-1 TAR RNA is a potential target for antisense oligonucleotides since it occurs at the 5'-end of all HIV-1 RNA transcripts and is regulated by the cognate protein Tat during transcriptional elongation.<sup>37–40</sup> The target region in HIV-1 TAR is a relatively short but chemically interesting RNA-construct, which consists of a trinucleotide UCU bulge and a

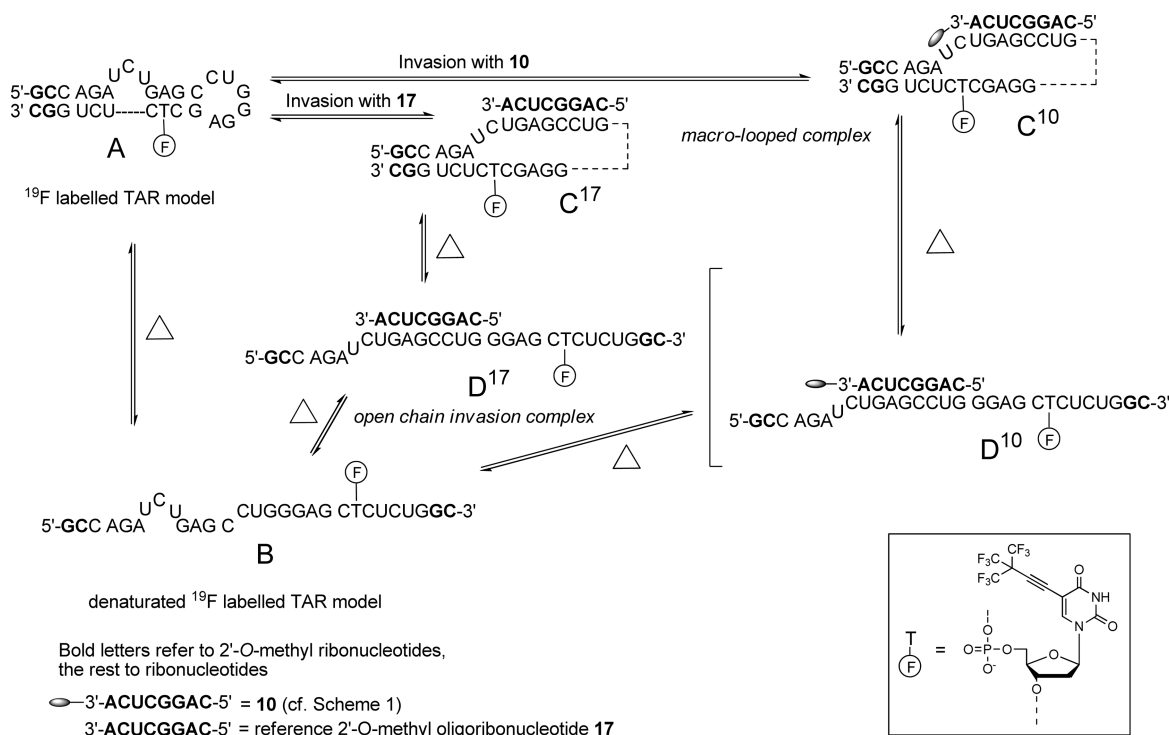
Received: February 24, 2011

Revised: June 14, 2011

Published: June 21, 2011

Scheme 1. Synthesis of Conjugates 10–16<sup>a</sup>


<sup>a</sup> Reagents and conditions: (i) TfaOMe, MeOH, Et<sub>3</sub>N; (ii) DMTrCl, Py, overall yields (from 1, 4 and 7), 3, 73%; 6, 59%; and 9, 51%; (iii) succinanhidride, DMAP, pyridine; (iv) LCAA-CPG, HATU, DIEA, DMF; (v) benzylamine, HATU, DIEA, DMF; (vi) acetic anhydride, lutidine, 1-methyl imidazole, THF; (vii) standard automated RNA synthesis; (ix) 0.1 mol L<sup>-1</sup> NaOMe in MeOH; (x) ammonolysis; (xi) RP HPLC conditions, a gradient elution from 10% to 40% acetonitrile in 0.1 mol L<sup>-1</sup> aq. Et<sub>3</sub>NH<sup>+</sup>AcO<sup>-</sup> over 25 min, Thermo ODS Hypersil column (250 × 4.6 mm, 5 μm) at a flow rate of 1.0 mL min<sup>-1</sup>.

 Scheme 2. Invasions of 8-Mer 2'-O-Methyl Oligoribonucleotide (17) and Its Neomycin-3'-conjugate (10) to the <sup>19</sup>F Labeled HIV-1 TAR RNA Model (A)


hairpin loop linked together by a tetranucleotide stem region. The essential elements for HIV-1 TAR targeting may, however,

be applied more generally to oligonucleotide-based drug design since related RNA-constructs exist in many biologically relevant

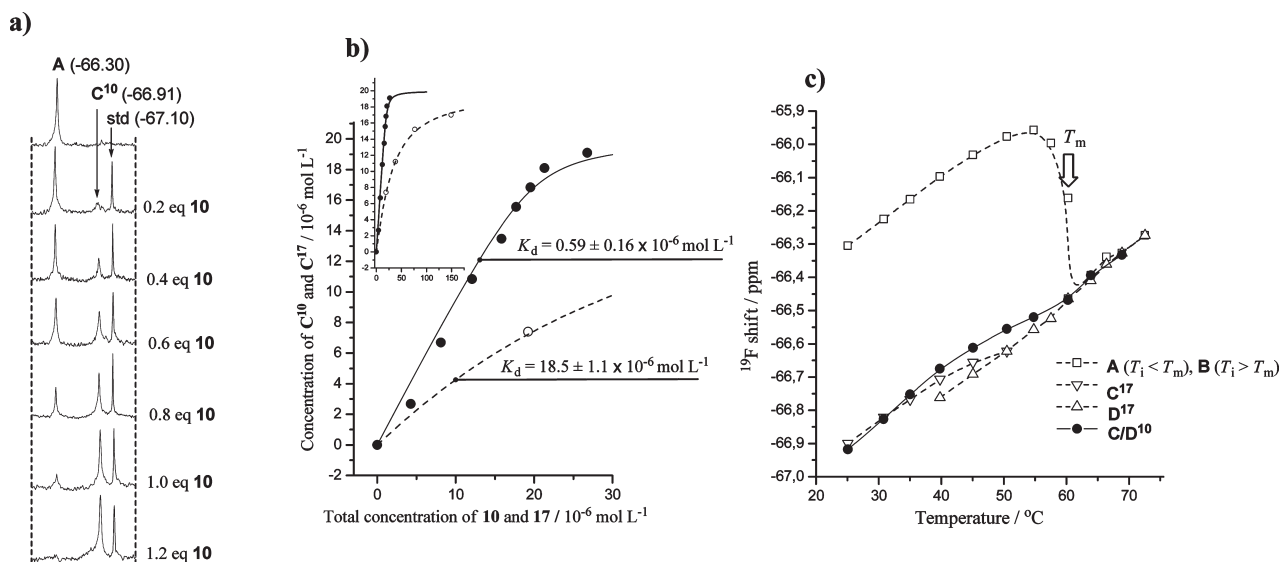


**Figure 1.** (a)  $^{19}\text{F}$  NMR spectra of A ( $20 \mu\text{mol L}^{-1}$  in  $25 \text{ mmol L}^{-1}$   $\text{NaH}_2\text{PO}_4$  buffered  $\text{H}_2\text{O}-\text{D}_2\text{O}$  (9:1, v/v, pH 6.5) in the presence of increasing concentrations of 10. 5-[4,4,4-Trifluoro-3,3-bis(trifluoromethyl)but-ynyl]-2'-deoxyuridine ( $10 \mu\text{mol L}^{-1}$ ) was used as an internal standard (std). (b) Titration curves obtained by integrals of  $^{19}\text{F}$  resonances in different concentrations of 10 (●) and 17 (○),  $\{[\text{C}^n] = [\text{A}_{\text{tot}}] \times \text{a relative } ^{19}\text{F} \text{ peak area } \text{C}^n/(\text{C}^n + \text{A})\}$ . (c)  $^{19}\text{F}$  shift versus temperature profiles. A, B, C<sup>17</sup>, D<sup>17</sup>, and C/D<sup>10</sup>; cf. Schemes 1 and 2.

RNAs. Among them are microRNAs, which recently have been reassessed as potential of antisense targets.<sup>41</sup> We have recently shown that neomycin induces invasion of a 2'-O-methyl oligoribonucleotide to a HIV-1 TAR model.<sup>42</sup> In the present study, neomycin, ribostamycin, and methyl neobiosamine have been covalently attached to the 3'-terminus of 2'-O-methyl oligoribonucleotides (10–16), and influence of the conjugated aminoglycosides on RNA invasion has been studied. As done previously, a  $^{19}\text{F}$  labeled HIV-1 TAR RNA model A (Scheme 2) has been used as a target, which allows monitoring of the secondary structural arrangement upon invasion by  $^{19}\text{F}$  NMR spectroscopy. For the preparation of the conjugates (10–16), a straightforward procedure was applied (Scheme 1). Partially protected aminoglycosides (3, 6, and 9), bearing the dimethoxytrityl protected primary hydroxyl group and trifluoroacetyl protected amino groups, were covalently attached to a LCAA CPG-support via succinyl linker. After capping of the remaining reactive functionalities, 2'-O-methyl oligoribonucleotide sequences were automatically elongated to these solid-supported aminoglycosides. A two-step procedure (1, NaOMe/MeOH; 2, ammonolysis) was used for the deprotection/release, to avoid  $O \rightarrow N$ -acyl migration on the aminoglycoside moieties. A relatively simple protecting group scheme may, hence, be utilized. For  $K_d$  determinations, a mixture of the  $^{19}\text{F}$  labeled HIV-1 TAR model was titrated by these conjugates. According to  $^{19}\text{F}$  NMR spectroscopic monitoring (Figure 1a), the neomycin moiety remarkably induces invasion of 2'-O-methyl oligoribonucleotides (Figure 1b). The right side (rings I, II, and III, i.e., ribostamycin) of the neomycin moiety also resulted in a slight enhancement, but influence of the left side (rings III and IV, i.e., biosamine) remained marginal (Table 2). The enhanced invasion was attributed to a formation of a stabilized macro-looped complex, by concurrent hybridization and binding of the neomycin moiety (Scheme 2 and Figure 1c). Interestingly, if the neomycin moiety is not appropriately available, the invasion may also follow a

mechanism, in which the first molar equivalent of the conjugate induces hybridization of the second.

## EXPERIMENTAL PROCEDURES

**General Remarks.** The NMR spectra of 3, 6, and 9 were recorded at 500 MHz. The chemical shifts are given in ppm from internal TMS and coupling constants in hertz. Peak assignments were supported by COSY and HSQC. The mass spectra of 3, 6, and 9 and oligonucleotide conjugates 10–16 were recorded by ESI ionization. Oligonucleotides 10–16 were assembled on an Applied Biosystems 392 DNA synthesizer using commercially available 2'-O-methyl ribonucleoside phosphoramidites. Standard RNA coupling protocol was followed. The  $^{19}\text{F}$  labeled TAR model (A) was prepared as previously described.<sup>42</sup> A Thermo Hypersil ODS column ( $250 \times 4.6 \text{ mm}$ ,  $5 \mu\text{m}$ ) at a flow rate of  $1 \text{ mL min}^{-1}$  was used for the RP HPLC purification of the conjugates (10–16). A gradient elution from 10% to 40% acetonitrile in  $0.1 \text{ mol L}^{-1} \text{Et}_3\text{NH}^+\text{AcO}^-$ -buffer over 25 min was used.

**$^{19}\text{F}$  NMR Spectroscopy.** Oligonucleotides (triethylammonium salts) were lyophilized to dryness and dissolved in  $25 \text{ mmol L}^{-1} \text{NaH}_2\text{PO}_4$ -buffer (pH 6.5) in  $\text{D}_2\text{O}-\text{H}_2\text{O}$  (1:9 v/v). For the titration experiments, conjugates were added as  $1 \text{ mmol L}^{-1}$  solutions to a  $20 \mu\text{mol L}^{-1}$  solution of  $^{19}\text{F}$  labeled HIV-1 TAR model (A). Prior to each spectroscopic detection, the mixtures were heated to  $90 \text{ }^\circ\text{C}$  for 1 min and then allowed to cool down to room temperature. Spectra were recorded at a frequency of 376.1 MHz on a Bruker Avance 400 MHz spectrometer. Typical experimental parameters were chosen as follows:  $^{19}\text{F}$  excitation pulse,  $12.6 \mu\text{s}$ ; acquisition time, 0.675 s; relaxation delay, 1.0 s; and usual number of scans, 2400 or 4800.  $^{19}\text{F}$  resonances were referenced relative to external  $\text{CCl}_3\text{F}$ . Sample temperature for the  $^{19}\text{F}$  shift versus temperature profiles (cf. Figure 1c) was calibrated by using known shifts of ethylene glycol at different temperatures.  $K_d$  values were calculated from relative peak areas of  $^{19}\text{F}$  resonance signals of the free HIV-1 TAR model (A) and

of the complexes (C) according to the following equations:  $K_d[C] = [A][ON]$ ,  $[A] + [C] = [A_{tot}]$ ,  $[ON] = [ON_{tot}] - [C] \rightarrow [C]^2 - ([A_{tot}] + [ON_{tot}] + K_d)[C] + [ON_{tot}][A_{tot}] = 0$ , where  $[C]$  = concentration of the invasion complex =  $X[A_{tot}]$ ,  $X$  = a relative  $^{19}\text{F}$  signal peak area (cf. Figure 1a) of the invasion complex,  $[A_{tot}]$  = the total concentration of A,  $[A]$  = concentration of free A,  $[ON_{tot}]$  = total concentration of the conjugate, and  $[ON]$  = concentration of the free conjugate. Titrations were additionally performed in the presence of the 5-[4,4,4-trifluoro-3,3-bis(trifluoromethyl)but-1-ynyl]-2'-deoxyuridine ( $10 \mu\text{mol L}^{-1}$ ) standard,<sup>43</sup> to which the peak areas were referenced.

**Thermal UV Denaturation Studies.** Absorbance versus temperature profiles (Supporting Information) were recorded at 260 nm on a Perkin-Elmer Lambda 35 UV–vis spectrometer equipped with a multiple cell holder and a Peltier temperature-controller. The temperature was changed at a rate of  $0.5 \text{ }^\circ\text{C}/\text{min}$  (from 20 to  $90 \text{ }^\circ\text{C}$ ). The measurements were performed in 25 mM  $\text{NaH}_2\text{PO}_4$  buffer (pH 6.5).  $T_m$  values were determined as the maximum of the first derivative of the melting curve.

**5'-O-(4,4'-Dimethoxytrityl)-1,3,2',6',2''',6'''-hexa-N-trifluoroacetylneomycin (3).** Triethylamine (3.6 mL, 26 mmol) and methyl trifluoroacetate (2.6 mL, 26 mmol) were added to neomycin trisulfate (7, 2.0 g, 2.2 mmol) in methanol (10 mL). The mixture was stirred overnight at room temperature and evaporated to dryness. Saturated  $\text{NaHCO}_3$  was added to the residue, and the crude product (2) was extracted with ethyl acetate. The organic layers were combined, dried over  $\text{Na}_2\text{SO}_4$ , filtered, and evaporated to dryness. The residue was further dried by coevaporation with dry pyridine and dissolved in dry pyridine, and then 4,4'-dimethoxytrityl chloride (0.80 g, 2.4 mmol) was added to the mixture. After overnight reaction, saturated  $\text{NaHCO}_3$  was added, and the product was extracted with ethyl acetate. The organic layers were combined, dried over anhydrous  $\text{Na}_2\text{SO}_4$ , filtered, and evaporated to dryness. The residue was purified by silica gel chromatography (10% MeOH, 1%  $\text{Et}_3\text{N}$  in  $\text{CH}_2\text{Cl}_2$ ) to yield 2.35 g (73%) of the product (3) as white foam.  $^1\text{H}$  NMR ( $\text{CD}_3\text{OD}$ , 500 MHz)  $\delta$ : 7.46 (m, 2H), 7.36–7.30 (m, 6H), 7.21 (m, 1H), 6.90 (m, 4H), 5.78 (d, 1H,  $J = 3.3$  Hz), 5.16 (d, 1H,  $J = 4.6$  Hz), 5.09 (d, 1H,  $J = 1.5$  Hz), 4.29 (dd, 1H,  $J = 4.8$  Hz, both), 4.21–4.20 (m, 2H), 4.14 (m, 1H), 4.11 (dd, 1H,  $J = 6.7$  Hz, both), 4.01 (m, 1H), 3.97 (m, 1H), 3.92 (m, 1H), 3.87 (dd, 1H,  $J = 9.9$  and 8.8 Hz), 3.80 (s, 6H), 3.75–3.63 (m, 5H), 3.60 (dd, 1H,  $J = 13.5$  and 7.4 Hz), 3.56–3.51 (m, 2H), 3.35–3.31 (m, 3H), 3.19 (dd, 1H,  $J = 10.5$  and 3.1 Hz), 2.00 (ddd, 1H,  $J = 12.9$  Hz, 4.2 and 4.2 Hz), 1.77 (ddd, 1H,  $J = 12.7$  Hz, each).  $^{13}\text{C}$  NMR ( $\text{CD}_3\text{OD}$ , 125 MHz)  $\delta$ : 157.93, 157.85, 145.0, 136.0, 135.6, 130.2, 129.9, 128.0, 127.4, 126.3, 112.7, 109.0, 97.6, 96.3, 87.4, 86.3, 81.9, 76.9, 75.6, 74.8, 73.0, 72.1, 71.5, 70.3, 69.8, 69.2, 67.1, 62.5, 54.3, 53.5, 51.3, 49.6, 49.1, 40.4, 39.6, 31.5 (Tfa related peaks not listed). HRMS(ESI): found 1515.3239,  $[\text{M} + \text{Na}]^+$  requires 1515.3265 (error 1.7 ppm).

**5'-O-(4,4'-Dimethoxytrityl)-1,3,2',6'-tetra-N-trifluoroacetylribostamycin (6).** Compound 6 was synthesized from 4 (as a disulfate salt, 0.25 g, 0.38 mmol) as described for the neomycin derivative 3 from 1 above. After silica gel chromatography (5% MeOH and 0.2%  $\text{Et}_3\text{N}$  in  $\text{CH}_2\text{Cl}_2$ ) 0.26 g (59%) of 6 was obtained as white foam.  $^1\text{H}$  NMR ( $\text{CD}_3\text{OD}$ , 500 MHz)  $\delta$ : 7.46 (m, 2H), 7.34 (m, 4H), 7.29 (m, 2H), 7.20 (m, 1H), 6.86 (m, 4H), 5.67 (d, 1H,  $J = 2.7$  Hz), 5.22 (d, 1H,  $J = 4.0$  Hz), 4.18–4.10 (m, 3H), 4.02–3.97 (m, 3H), 3.92 (m, 1H), 3.81 (m, 1H), 3.78 (s, 6H), 3.76–3.64 (m, 4H), 3.60 (m, 2H), 3.30–3.25 (m, 2H), 3.23 (dd, 1H,  $J = 10.2$  and 3.8 Hz), 2.01 (ddd, 1H,  $J = 12.9$  Hz, 4.2

and 4.2 Hz), 1.75 (ddd, 1H,  $J = 12.8$  Hz each).  $^{13}\text{C}$  NMR ( $\text{CD}_3\text{OD}$ , 125 MHz)  $\delta$ : 158.7, 145.0, 136.0, 135.8, 130.02, 129.95, 128.0, 127.4, 126.3, 112.7, 109.2, 96.6, 86.7, 83.2, 76.4, 75.5, 72.9, 72.1, 70.9, 70.2, 70.1, 63.1, 54.3, 53.8, 49.7, 49.2, 40.5, 31.5 (Tfa related peaks not listed). HRMS(ESI): found 1163.2786,  $[\text{M} + \text{Na}]^+$  requires 1163.2771 (error 1.3 ppm).

**Methyl-2',6'-Bis-N-trifluoroacetyl Neobiosamine B (9).** Compound 9 was synthesized from 7 (as free amine,  $\beta:\alpha = 0.77:0.23$ , 0.63 g, 1.9 mmol) as described for the neomycin derivative 3 from 1 above, but 2 mol equiv of DMTrCl was used. After silica gel chromatography (5% MeOH and 0.2%  $\text{Et}_3\text{N}$  in  $\text{CH}_2\text{Cl}_2$ ), 0.63 g (51%) of 8 (pure  $\beta$  isomer) was obtained as white foam.  $^1\text{H}$  NMR ( $\text{CD}_3\text{OD}$ , 500 MHz)  $\delta$ : 7.60 (m, 2H), 7.47 (m, 4H), 7.28 (m, 2H), 7.20 (m, 1H), 6.87 (m, 4H), 5.36 (b, 1H), 4.36 (d, 1H,  $J = 7.3$  Hz), 4.34 (b, 1H), 4.27 (b, 1H), 4.20 (dd, 1H,  $J = 6.8$  and 6.7 Hz), 4.07 (b, 1H), 3.77 (s, 6H), 3.71 (dd, 1H,  $J = 12.8$  and 8.8 Hz), 3.62 (b, 1H), 3.54 (b, 1H), 3.52 (dd,  $J = 12.8$  and 4.9 Hz), 3.36 (s, 3H), 3.32 (b, 1H), 3.18 (m, 2H), 2.33 (b, 1H).  $^{13}\text{C}$  NMR ( $\text{CD}_3\text{OD}$ , 125 MHz)  $\delta$ : 157.4, 144.4, 135.3, 135.0, 128.7, 127.0, 125.9, 124.9, 111.3, 111.1, 100.2, 96.3, 85.4, 75.3, 69.9, 69.6, 67.8, 67.5, 65.6, 60.7, 54.1, 52.8, 50.1 (Tfa related peaks not listed). HRMS(ESI): found 842.2415,  $[\text{M} + \text{Na}]^+$  requires 841.2383 (error 3.8 ppm).

**Synthesis of the Conjugates 10–14.** Succinamide (3.4 mg, 33  $\mu\text{mol}$ ) and a catalytic amount of DMAP were added to a mixture of 3, 6, or 9 (33  $\mu\text{mol}$ , each) in dry pyridine (0.50 mL). The mixtures were stirred overnight at ambient temperature and evaporated to dryness. (According to MS(ESI), the crude product mixtures also contained multiply succinated side products in addition to monosuccinates.) The residues were dissolved in DMF (1.0 mL), and HATU (25 mg, 67  $\mu\text{mol}$ ), DIEA (23  $\mu\text{L}$ , 130  $\mu\text{mol}$ ), and LCAA-CPG support (100 mg) were added to the mixtures. After overnight shaking, the suspensions were filtered, and the supports were washed with DMF and  $\text{CH}_2\text{Cl}_2$  and dried under vacuum. The potential unreacted carboxylic acid groups on the supports were capped by amide bond formation. Accordingly, the supports were suspended in DMF (1.0 mL), and benzylamine, HATU, and DIEA were added to the suspensions. After overnight shaking, the supports were filtered, washed with DMF and  $\text{CH}_2\text{Cl}_2$ , and dried under vacuum. The unreacted hydroxyl groups of the solid supported aminoglycosides and the unreacted amino groups of the initial support were then acetylated by double syringe method using a mixture of acetic anhydride, lutidine, and *N*-methyl imidazol in THF (5:5:8:82, v/v/v/v, for 15 min at  $25 \text{ }^\circ\text{C}$ ). After acetylation, the resins were washed with THF and  $\text{CH}_2\text{Cl}_2$  and dried under vacuum. A small aliquot of each resin was analyzed by the DMTr-cation assay. Loadings of 17  $\mu\text{mol g}^{-1}$  (neomycin resin), 14  $\mu\text{mol g}^{-1}$  (ribostamycin resin), and 19  $\mu\text{mol g}^{-1}$  (methyl neobiosamine resin) were obtained. The appropriate oligonucleotide chains were then assembled (0.5  $\mu\text{mol}$  scale) by standard automated RNA protocol. After chain assembly, supports were treated with 0.1 M NaOMe in MeOH (1.0 mL, for 2 h at  $25 \text{ }^\circ\text{C}$ ) and filtered. One molar aqueous ammonium chloride (100  $\mu\text{L}$ ) was added to the filtrates, and the mixtures were evaporated to dryness. Supports and the filtrates were combined and treated with saturated ammonia for 15 h at  $55 \text{ }^\circ\text{C}$ . Finally, the mixtures were filtered, evaporated to dryness, dissolved in water, and purified by RP HPLC [a gradient elution from 10% to 40% acetonitrile in 0.1 mol  $\text{L}^{-1}$  aq.  $\text{Et}_3\text{NH}^+\text{AcO}^-$  over 25 min, Thermo ODS Hypersil column (250  $\times$  4.6 mm, 5  $\mu\text{m}$ ) at a flow rate of 1.0 mL  $\text{min}^{-1}$ ; an example of the RP HPLC chromatogram is shown in Scheme 1].

Table 1

conjugate	observed mass	calculated mass
10	1646.9 <sup>a</sup>	1646.4
11	909.0 <sup>b</sup>	909.0
12	1666.9 <sup>c</sup>	1666.4
13	1136.3 <sup>a</sup>	1136.3
14	816.7 <sup>a</sup>	816.7
15	1566.9 <sup>a</sup>	1566.8
16	1501.8 <sup>a</sup>	1501.8

<sup>a</sup> [M - 2H]<sup>2-</sup>. <sup>b</sup> [M - 4H]<sup>4-</sup>. <sup>c</sup> [M + K - 3H]<sup>2+</sup>.

The isolated products were desalted and lyophilized to dryness. Authenticity of the isolated products 10–16 was verified by MS (ESI) spectroscopy (Table 1).

## RESULTS AND DISCUSSION

**Synthesis of the Aminoglycoside 3'-Conjugates of 2'-O-Methyl Oligoribonucleotides (10–16).** Synthesis of the conjugates (10–16) is described in Scheme 1. The protecting group scheme was simplified by using a one-pot anchoring/protection procedure of partially protected aminoglycosides (3, 6, and 9). Neomycin (1), ribostamycin (4), and methyl neobiosamine (7) were *N*-trifluoroacetylated (2, 5, and 8), and the primary hydroxyl group was selectively protected by the 4,4'-dimethoxytrityl group. Compounds (3, 6, or 9) were then treated with one molar equivalent of succinylhydride (iii), the crude products were attached to the LCAA-CPG support (iv), and the potential free carboxyl and hydroxyl groups on the supports were capped by amide bond formation (v) and acetylation (vi), respectively. An automated oligonucleotide chain elongation (vii) was successfully performed on the obtained aminoglycoside supports. In order to avoid potential *O*→*N*-acyl migration on the aminoglycoside moieties, a two-step deprotection-procedure was performed. The solid-supported conjugates were subjected to a mixture of NaOMe in methanol (ix, ester cleavage), and then the deprotection was continued by ammonolysis (x, amide cleavage). The sodium methoxide pretreatment favors transesterification, in which the trifluoroacetamides stay intact. According to RP HPLC chromatograms (an example is shown in Scheme 1) and MS (ESI) spectra (Table 1), products were successfully obtained without *O*→*N*-acyl migration.

**Invasion of the Conjugates to the <sup>19</sup>F Labeled TAR Model (A).** <sup>19</sup>F is biologically nonexistent and has an NMR-sensitive nucleus (83% compared to <sup>1</sup>H), which additionally offers wide chemical shift dispersion. These properties make the <sup>19</sup>F nucleus a useful probe for the monitoring of conformational transitions in RNA.<sup>42–51</sup> Closely related to this work, 2'-deoxy-2'-fluoronucleosides incorporated in RNA have been used for the monitoring RNA-aminoglycoside interactions,<sup>47</sup> and 2,4-difluorotoluene nucleosides have been used for the quantification of hairpin/hairpin and duplex/hairpin equilibria of self-complementary RNAs.<sup>49</sup> We have recently demonstrated the applicability of <sup>19</sup>F NMR spectroscopy to the monitoring of RNA invasion, by studying the binding of 2'-*O*-methyl oligoribonucleotides to the <sup>19</sup>F labeled HIV-1 TAR RNA model A.<sup>42</sup> The 5-[4,4,4-trifluoro-3,3-bis(trifluoromethyl)but-1-ynyl]-2'-deoxyuridine sensor<sup>43</sup> within the model decreases the stability of the four nucleotide stem between the loop and the UCU-bulge ( $\Delta T_m = -2.7$  °C), slightly facilitating the invasion. The model (A) is, hence, useful

Table 2.<sup>a</sup>

oligonucleotide	$K_d$ ( $\mu\text{mol L}^{-1}$ )
10	0.59 ± 0.16
11	4.9 ± 1.5
12	0.32 ± 0.22
13	37.0 ± 2.0
15	3.8 ± 0.7
16	25.0 ± 0.4
17	18.5 ± 1.1
17 + 14 (1:1, <i>n/n</i> )	3.6 ± 0.8

<sup>a</sup> Each  $K_d$  is simplified to stoichiometric (1:1) complexes.

for comparative evaluation of the affinities of different invader oligonucleotides. A distinct <sup>19</sup>F resonance signal from that referring to the initial hairpin structure may be obtained, when a structural change, such as invasion (C/D) or thermal denaturation (B), takes place. Additionally, temperature-dependent behavior of the complexes may be followed by <sup>19</sup>F shift vs temperature profiles since the potential macro-looped (C) and the open-chain invasion complex (D) may, in a favorable case, result in <sup>19</sup>F signals with different resonance shifts (Figure 1c). Note that there is a linear temperature-dependent <sup>19</sup>F shift downfield with the slope 0.014 ppm K<sup>-1</sup>. Deviations from this passive shift refer to structural changes in RNA. In the present study, model A was titrated with conjugates 10–13, (14 + 17), 15, and 16, and their invasion efficiency was evaluated by <sup>19</sup>F NMR spectroscopy. We recently showed that invasion of 2'-*O*-methyl oligoribonucleotide 17 (Scheme 2) to A may be induced by the presence of neomycin (as a discrete molecule).<sup>42</sup> Therefore, neomycin, when covalently attached to the same 2'-*O*-methyl oligoribonucleotide (10), may be expected to result in a cooperative effect, in which the complex is stabilized by concurrent hybridization and binding of the neomycin moiety. The site-specific binding of neomycin occurs below the bulged nucleotides of the native HIV-1 TAR region through the minor groove.<sup>25</sup> Stabilization of the complex should, hence, be based on the formation of the macro-looped complex (C<sup>10</sup>) since the open-chain invasion complex (D<sup>10</sup>) contains only the canonical double strand with a modest affinity to aminoglycosides. <sup>19</sup>F NMR spectra during the titration of A with 10 is shown in Figure 1a, and the titration curve recording the relative <sup>19</sup>F peak areas is shown in Figure 1b. As seen from Figure 1b, conjugate 10 provides a significantly enhanced invasion compared to that obtained by unmodified 2'-*O*-methyl oligoribonucleotide 17. Fitting the titration curve to the stoichiometric (1:1) complex formation, gave  $K_d = 0.59 \pm 0.16 \mu\text{mol L}^{-1}$  with 10, whereas  $K_d = 18.5 \pm 1.1 \mu\text{mol L}^{-1}$  was obtained with 17. An interesting observation was additionally done, when the mixture of the complex C/D<sup>10</sup> was heated. The <sup>19</sup>F shift vs temperature profile of the complex (C/D<sup>10</sup>) followed the prolonged downfield curve of the complex (C/D<sup>17</sup>) with unmodified 2'-*O*-methyl oligoribonucleotide 17 (Figure 1c). We have previously concluded that the downfield curve (∇ in Figure 1c) refers to the macrolooped complex (C<sup>17</sup>) and the upfield curve (Δ in Figure 1c) to the open-chain invasion complex (D<sup>17</sup>).<sup>42</sup> The prolonged downfield curve (●) refers to neomycin binding and is consistent with the expectation that the enhanced invasion is related to the stabilized macro-looped complex (C<sup>10</sup>).

Invasion by the other conjugates was similarly studied (see titration curves in the Supporting Information), and the  $K_d$

values for each complex are listed in Table 2. Comparing  $K_d$  of  $C^{11}$  ( $4.9 \pm 1.5 \mu\text{mol L}^{-1}$ ) to that of  $C^{10}$  ( $0.59 \pm 0.16 \mu\text{mol L}^{-1}$ ) shows that shifting of the 2'-*O*-methyl oligoribonucleotide sequence by one nucleotide (C at 5'-end deleted and G at 3'-end added) significantly decreases the affinity. More interestingly, the titration curve obtained by  $C^{11}$  hardly follows 1:1-complex formation, but the saturation is deviated to a 2:1-stoichiometry. An explanation to this phenomenon is that the above-mentioned cooperative effect could not be gained with **11** but that the first molar equivalent of the conjugate may induce invasion of the second. In order to evaluate the efficiency of this ternary mechanism, titration was additionally performed with a 1:1-mixture of unmodified octamer **17** and neomycin conjugate **14**, which with the short CAG-strand cannot alone invade **A** (cf. **13** below). Conjugate **14**, however, does induce the invasion of **17** of **A**, for which  $K_d = 3.6 \pm 0.8 \mu\text{mol L}^{-1}$  (simplified to 1:1-complex formation) may be determined. This verifies that invasion with conjugate **11** may be induced in a ternary manner. The ternary induction may partly take place also with **10** (or with other conjugates as well), but the titration profile may be more overlapped by that of the stoichiometric (1:1) complex formation. In order to avoid potential structural constraints for the cooperative recognition, conjugate **12**, bearing a flexible polyethylene glycol spacer between the neomycin moiety and 2'-*O*-methyl oligoribonucleotide, was targeted to **A**. As expected, the more flexible spacer facilitates cooperativity, and a higher affinity ( $K_d = 0.32 \pm 0.22 \mu\text{mol L}^{-1}$ ) compared to that of **10** was obtained. Noteworthy, this strongly stoichiometric complex formation approach's limitations can be reliably detected by the adopted method (based on integrals of  $^{19}\text{F}$  resonance signals). Importance of the left (biosamine) and right (ribostamycin) sides of the neomycin moiety may be seen in  $K_d$  values of  $C^{16}$  and  $C^{17}$ . The affinities were expectedly weaker than that of **10** ( $C^{10}$ :  $K_d = 0.59 \pm 0.16 \mu\text{mol L}^{-1}$ ), and the ribostamycin moiety still promotes invasion ( $C^{13}$ :  $K_d = 3.8 \pm 0.7 \mu\text{mol L}^{-1}$ ), but influence of the biosamine moiety ( $C^{14}$ :  $K_d = 25 \pm 0.4 \mu\text{mol L}^{-1}$ ) to that of **17** ( $C^{17}$ :  $K_d = 18.5 \pm 1.1 \mu\text{mol L}^{-1}$ ) was marginal (slightly negative). Titration with neomycin conjugate **13**, bearing a short pentanucleotide sequence, resulted in a broad and fragmented signal into the  $^{19}\text{F}$  NMR spectrum. This is a consequence of weak hybridization, in which unspecific binding of the neomycin moiety (conjugate in excess) already predominates. Only a weak invasion ( $K_d = 36.9 \pm 2.0 \mu\text{mol L}^{-1}$  simplified to stoichiometric 1:1-complex formation) was observed. Mixtures of the complexes were also heated to provide the  $^{19}\text{F}$  shift vs temperature profiles (see Supporting Information). The stable complex  $C^{12}$  expectedly followed the prolonged downfield curve similar to  $C^{10}$  (cf. Figure 1c), and a slightly prolonged downfield curve was obtained also with  $C^{11}$ . Similar downfield shifting was not obtained with complexes ( $C^{15}$  and  $C^{16}$ ) of ribostamycin and neobiosamine conjugates. Consistent with  $^{19}\text{F}$  shift vs temperature profiles, complexes  $C^{10-12}$  were stable upon heating (at a temperature lower than  $T_m$ ), but equilibrium between **A** and **15** or **16** was dynamic, and hence, the amount of complexes  $C^{15}$  or  $C^{16}$  decreased upon heating. UV-melting profiles of the complexes were also measured. Noteworthy, these are performed in a diluted  $2 \mu\text{mol L}^{-1}$  solution of **A** in the presence of the conjugates (**10**, **11**, **14** + **17**, **15**, and **16**, 2 equiv; **12**, 1 equiv; and **13**, 5 equiv), in which the weak complexes are mainly dissociated. The only conjugate which resulted in an increased  $T_m$  was **12** (1 equiv,  $T_m = 62.7^\circ\text{C}$ ; **A**,  $T_m = 60.7^\circ\text{C}$ ). No change

or a slightly decreased  $T_m = 59.2\text{--}60.6^\circ\text{C}$  was observed with other conjugates.

## CONCLUSIONS

Aminoglycoside (neomycin, ribostamycin, and methyl neobiosamine) 3'-conjugates of 2'-*O*-methyl oligoribonucleotides have been synthesized entirely on a solid phase, and their invasion efficiency to a  $^{19}\text{F}$  labeled HIV-1 TAR model has been evaluated by  $^{19}\text{F}$  NMR spectroscopy. In addition to the determined  $K_d$ -values,  $^{19}\text{F}$  shift versus temperature profiles of the complexes have been measured. A significantly enhanced invasion in the presence of the neomycin moiety (conjugates **10** and **12**) has been obtained. Enhancement has been concluded to be involved in the stabilized macro-looped complex, which allows concurrent hybridization and binding of the neomycin moiety. Aminoglycoside-promoted RNA-invasion has hence been verified, which may give new ideas for the oligonucleotide-based RNA targeting.

## ASSOCIATED CONTENT

**S** Supporting Information.  $^1\text{H}$  NMR and  $^{13}\text{C}$  NMR spectra, RP HPLC chromatograms, titration curves,  $^{19}\text{F}$  shift vs the temperature profile, and UV-melting curves. This material is available free of charge via the Internet at <http://pubs.acs.org>.

## AUTHOR INFORMATION

### Corresponding Author

\*Fax: +35823336700. E-mail: [pamavi@utu.fi](mailto:pamavi@utu.fi).

## ACKNOWLEDGMENT

The financial support from the Academy of Finland is gratefully acknowledged.

## REFERENCES

- (1) Davies, J., Gorini, L., and Davis, B. D. (1965) Misreading of RNA codewords induced by aminoglycoside antibiotics. *Mol. Pharmacol.* 1, 93–106.
- (2) Moazed, D., and Noller, H. F. (1987) Interaction of antibiotics with functional sites in 16S ribosomal RNA. *Nature* 327, 389–394.
- (3) Francois, B., Russell, R. J. M., Murray, J. B., Aboul-ela, F., Masquida, B., Vicens, Q., and Westhof, E. (2005) Crystal structures of complexes between aminoglycosides and decoding site oligonucleotides: role of the number of rings and positive charges in the specific binding leading to miscoding. *Nucleic Acid Res.* 33, 5677–5690.
- (4) Recht, M. I., Fourmy, D., Blanchard, S. C., Dahlquist, K. D., and Puglisi, J. D. (1996) RNA sequence determinants for aminoglycoside binding to an A-site rRNA model oligonucleotide. *J. Mol. Biol.* 261, 421–436.
- (5) Purohit, P., and Stern, S. (1994) Interaction of a small RNA with antibiotic and RNA ligands of the 30S subunit. *Nature* 370, 659–662.
- (6) Von Ahsen, U., and Noller, H. F. (1993) Footprinting the sites of interaction of antibiotics with catalytic group I intron RNA. *Science* 260, 1500–1503.
- (7) Von Ahsen, U., Davies, J., and Schroeder, R. (1991) Antibiotic inhibition of group I ribozyme function. *Nature* 353, 368–370.
- (8) Herman, T. (2005) Drugs targeting the ribosome. *Current Opin. Struct. Biol.* 15, 355–366.
- (9) Hoch, I., Berens, C., Westhof, E., and Schroeder, R. (1998) Antibiotic inhibition of RNA catalysis: Neomycin B binds to the catalytic core of the td group I intron displacing essential metal ions. *J. Mol. Biol.* 282, 557–569.

- (10) Mikkelsen, N. E., Brannval, M., Virtanen, A., and Kirsebom, L. A. (1999) Inhibition of RNase P RNA cleavage by aminoglycosides. *Proc. Natl. Acad. Sci. U.S.A.* 96, 6155–6160.
- (11) Earnshaw, D. J., and Gait, M. J. (1998) Hairpin ribozyme cleavage catalyzed by aminoglycoside antibiotics and the polyamine spermine in the absence of metal ions. *Nucleic Acid Res.* 26, 5551–5561.
- (12) Tor, Y., Hermann, T., and Westhof, E. (1998) Deciphering RNA recognition: aminoglycoside binding to the hammerhead ribozyme. *Chem. Biol.* 5, 277–283.
- (13) Stage, T. K., Hertel, K. J., and Uhlenbeck, O. C. (1995) Inhibition of the hammerhead ribozyme by neomycin. *RNA* 1, 95–101.
- (14) ClouDET-d'Orval, B., Stage, T. K., and Uhlenbeck, O. C. (1995) Neomycin inhibition of the hammerhead ribozyme involves ionic interactions. *Biochemistry* 34, 11186–11190.
- (15) Chia, J. S., Wu, H. L., Wang, H. W., Chen, D. S., and Chen, P. J. (1997) Inhibition of hepatitis delta virus genomic ribozyme self-cleavage by aminoglycosides. *J. Biomed. Sci.* 4, 208–216.
- (16) Tok, J. B. H., Cho, J., and Rando, R. R. (1999) Aminoglycoside antibiotics are able to specifically bind the 5'-untranslated region of thymidylate synthase messenger RNA. *Biochemistry* 38, 199–206.
- (17) Mei, H.-Y., Galan, A. A., Halim, N. S., Mack, D. P., Morelan, D. W., Sanders, K. B., Truong, H. N., and Czarnik, A. W. (1995) Inhibition of an HIV-1 Tat-derived peptide binding to TAR RNA by aminoglycoside antibiotics. *Bioorg. Med. Chem. Lett.* 5, 27552760.
- (18) Zapp, M. L., Stern, S., and Green, M. R. (1993) Small molecules that selectively block RNA binding of HIV-1 rev protein inhibit rev function and viral production. *Cell* 74, 969–978.
- (19) Tam, V. K., Kwong, D., and Tor, Y. (2007) Fluorescent HIV-1 dimerization initiation site: design, properties, and use for ligand discovery. *J. Am. Chem. Soc.* 129, 3257–3266.
- (20) Ennifar, E., Paillart, J.-C., Bodlenner, A., Walter, P., Weibel, J.-M., Aubertin, A.-M., Pale, P., Dumas, P., and Marquet, R. (2006) Targeting the dimerization initiation site of HIV-1 RNA with aminoglycosides: from crystal to cell. *Nucleic Acid Res.* 34, 2328–2339.
- (21) Arya, D. P., and Coffee, R. L., Jr. (2000) DNA triple helix stabilization by aminoglycoside antibiotics. *Bioorg. Med. Chem. Lett.* 10, 1897–1899.
- (22) Arya, D. P., Xue, L., and Tennant, P. (2003) Combining the best in triplex recognition: synthesis and nucleic acid binding of a BQQ-neomycin conjugate. *J. Am. Chem. Soc.* 125, 8070–8071.
- (23) Arya, D. P., Coffee, R. L., Jr., and Charles, I. (2001) Neomycin induced hybrid triplex formation. *J. Am. Chem. Soc.* 123, 11093–11094.
- (24) Thomas, J., and Hergenrother, P. J. (2008) Targeting RNA with small molecules. *Chem. Rev.* 108, 1171–1224.
- (25) Wang, S., Huber, P. W., Cui, M., Czarnik, A. W., and Mei, H.-Y. (1998) Binding of neomycin to the TAR element of HIV-1 RNA induces dissociation of Tat protein by an allosteric mechanism. *Biochemistry* 37, 5549–5557.
- (26) Blount, K. F., Zhao, F., Hermann, T., and Tor, Y. (2005) Conformational constraint as a means for understanding RNA-aminoglycoside specificity. *J. Am. Chem. Soc.* 127, 9818–9829.
- (27) Zamecnik, P. C., and Stephenson, M. L. (1978) Inhibition of Rous sarcoma virus replication and cell transformation by a specific oligodeoxynucleotide. *Proc. Natl. Acad. Sci. U.S.A.* 75, 280–284.
- (28) Stephenson, M. L., and Zamecnik, P. C. (1978) Inhibition of Rous sarcoma viral RNA translation by a specific oligodeoxyribonucleotide. *Proc. Natl. Acad. Sci. U.S.A.* 75, 285–288.
- (29) Napoli, S., Carbone, G. M., Catapano, C., Shaw, N., and Arya, D. P. (2005) Neomycin improves cationic lipid-mediated transfection of DNA in human cells. *Bioorg. Med. Chem. Lett.* 15, 3467–3469.
- (30) Irudayasamy, C., Xi, H., and Arya, D. P. (2007) Sequence-specific targeting of RNA with an oligonucleotide-neomycin conjugate. *Bioconjugate Chem.* 18, 160–169.
- (31) Riguet, E., Tripathi, S., Désire, J., Pandey, V. N., and Décout, J.-L. (2004) A peptide nucleic acid-neamine conjugate that targets and cleaves HIV-1 TAR RNA inhibits viral replication. *J. Med. Chem.* 47, 4806–4809.
- (32) Chaubey, B., Tripathi, S., Désire, J., Baussanne, I., Décout, J.-L., and Pandey, V. N. (2007) Mechanism of RNA cleavage catalyzed by sequence specific polyamide nucleic acid-neamine conjugate. *Oligonucleotides* 17, 302–313.
- (33) Ketomäki, K., and Virta, P. (2008) Synthesis of aminoglycoside conjugates of 2'-O-methyl oligoribonucleotides. *Bioconjugate Chem.* 19, 766–777.
- (34) Kiviniemi, A., Virta, P., and Lönnberg, H. (2010) Solid-supported synthesis and click conjugation of 4'-C-alkyne functionalized oligodeoxyribonucleotides. *Bioconjugate Chem.* 21, 1890–1901.
- (35) Kiviniemi, A., Virta, P., and Lönnberg, H. (2008) Utilization of intrachain 4'-C-azidomethylthymidine for preparation of oligodeoxyribonucleotide conjugates by click chemistry in solution and on a solid support. *Bioconjugate Chem.* 19, 1726–1734.
- (36) Mei, H., Xing, L., Cai, L., Hong-Wei, J., Zhao, P., Yang, Z.-J., Zhang, L.-R., and Zhang, L.-H. (2008) Studies on the synthesis of neamine-dinucleosides and neamine-PNA conjugates and their interaction with RNA. *Bioorg. Med. Chem. Lett.* 18, 5355–5358.
- (37) Vickers, T., Baker, B. F., Cook, P. D., Zounes, M., Buckheit, R. W., Jr., Germany, J., and Ecker, D. J. (1991) Inhibition of HIV-LTR gene expression by oligonucleotides targeted to the TAR element. *Nucleic Acids Res.* 19, 3359–3368.
- (38) Ecker, D. J., Vickers, T. A., Bruce, T. W., Freier, S. M., Jenison, R. D., Manoharan, M., and Zounes, M. (1992) Pseudo-half-knot formation with RNA. *Science* 257, 958–961.
- (39) Mestre, B., Arzumanov, A., Singh, M., Boulme, F., Litvak, S., and Gait, M. J. (1999) Oligonucleotide inhibition of the interaction of HIV-1 Tat protein with the trans-activation responsive region (TAR) of HIV RNA. *Biochim. Biophys. Acta* 1445, 86–98.
- (40) Arzumanov, A., Walsh, A. P., Rajwanshi, V. K., Kumar, R., Wengel, J., and Gait, M. J. (2001) Inhibition of HIV-1 Tat-dependent trans activation by steric block chimeric 2'-O-methyl/LNA oligoribonucleotides. *Biochemistry* 40, 14645–14654.
- (41) Kota, S. K., and Balasubramanian, S. (2010) Cancer therapy via modulation of micro RNA levels: a promising future. *Drug Discovery Today* 15, 733–740.
- (42) Kiviniemi, A., and Virta, P. (2010) Characterization of RNA invasion by <sup>19</sup>F NMR spectroscopy. *J. Am. Chem. Soc.* 132, 8560–8562.
- (43) Barhate, N. B., Barhate, R. N., Cekan, P., Drobny, G., and Th. Sigurdsson, S. (2008) A nonafluoro nucleoside as a sensitive <sup>19</sup>F NMR probe of nucleic acid conformation. *Org. Lett.* 10, 2745–2747.
- (44) Kreutz, C., Kählig, H., Konrat, R., and Micura, R. (2005) Ribose 2'-F labeling: A simple tool for the characterization of RNA secondary structure equilibria by <sup>19</sup>F NMR spectroscopy. *J. Am. Chem. Soc.* 127, 11558–11559.
- (45) Olsen, G. L., Edwards, T. E., Deka, P., Varani, G., Sigurdsson, S. Th., and Drobny, G. P. (2005) Monitoring tat peptide binding to TAR RNA by solid-state <sup>31</sup>P-<sup>19</sup>F REDOR NMR. *Nucleic Acid Res.* 33, 3447–3454.
- (46) Hennig, M., Munzáröva, M. L., Bermel, W., Scott, L. G., Sklenár, V., and Williamson, J. R. (2006) Measurement of long-range <sup>1</sup>H-<sup>19</sup>F scalar coupling constants and their glycosidic torsion dependence in 5-fluoropyrimidine-substituted RNA. *J. Am. Chem. Soc.* 128, 5851–5858.
- (47) Kreutz, C., Kählig, H., Konrat, R., and Micura, R. (2006) A General approach for the identification of site-specific RNA binders by <sup>19</sup>F NMR spectroscopy: Proof of concept. *Angew. Chem., Int. Ed.* 45, 3450–3453.
- (48) Hennig, M., Scott, L. G., Sperling, E., Bermel, W., and Williamson, J. R. (2007) Synthesis of 5-fluoropyrimidine nucleotides as sensitive NMR probes of RNA structure. *J. Am. Chem. Soc.* 129, 14911–14921.
- (49) Graber, D., Moroder, H., and Micura, R. (2008) <sup>19</sup>F NMR spectroscopy for the analysis of RNA secondary structure populations. *J. Am. Chem. Soc.* 130, 17230.

(50) Tanabe, K., Sugiura, M., and Nishimoto, S. (2010) Monitoring of duplex and triplex formation by  $^{19}\text{F}$  NMR using oligonucleotides possessing 5-fluorodeoxyuridine unit as  $^{19}\text{F}$  signal transmitter. *Bioorg. Med. Chem.* 18, 6690–6694.

(51) Moumné, R., Pasco, M., Prost, E., Lecourt, T., Micouin, L., and Tisné, C. (2010) Fluorinated diaminocyclopentanes as chiral sensitive NMR probes of RNA structure. *J. Am. Chem. Soc.* 132, 13111–13113.